Membrane localization and dynamics of Nile Red: Effect of cholesterol

Soumi Mukherjee, H. Raghuraman, Amitabha Chattopadhyay *

Centre for Cellular and Molecular Biology, Uppal Road, Hyderabad 500 007, India

Abstract

The organization and dynamics of the hydrophobic fluorescent probe Nile Red incorporated in DOPC vesicles containing varying amounts of cholesterol has been monitored utilizing fluorescence-based approaches which include the red edge excitation shift (REES) approach and the parallax method for depth determination. Our results show that the fluorescence emission maximum, intensity, polarization, and lifetime of Nile Red vary with the cholesterol content of the membrane. Interestingly, Nile Red exhibits significant REES independent of the presence of cholesterol. This indicates that Nile Red is localized in a motionally restricted environment in the membrane. This is supported by analysis of membrane penetration depth of Nile Red using the parallax method which points out to a membrane interfacial localization of Nile Red. These results could be useful in analyzing membrane organization and heterogeneity in natural membranes using Nile Red.
© 2006 Elsevier B.V. All rights reserved.

1. Introduction

Fluorescent probes have proved to be very useful in membrane biology due to their ability to monitor membrane organization and dynamics at increasing spatiotemporal resolution due to their high sensitivity, suitable time resolution, and multiplicity of measurable parameters [1]. A major criterion of a fluorescent membrane probe is the sensitivity of its fluorescence to environmental factors. Nile Red (9-diethylamino-5H-benzo[α]phenoxazine-5-one), an uncharged phenoxazone dye (see inset of Fig. 1a), is such a probe whose fluorescence properties are altered by the polarity of its immediate environment due to a large change in dipole moment upon excitation [2–5]. This large change in dipole moment has been attributed to charge separation between the diethylamino group which acts as the electron donor and the quinoid part of the molecule which serves as the electron acceptor.

Nile Red has been used as a fluorescent probe for monitoring hydrophobic surfaces in proteins [6], protein–detergent complexes [7], and as a lipid stain in membranes [8–10]. It has also been used for monitoring organization, fluctuation, and heterogeneity in membranes, specifically for membranes containing cholesterol [8,11,12]. Cholesterol plays a crucial role in membrane organization, dynamics, function and sorting [13,14]. It is often found distributed non-randomly in domains or pools in biological and model membranes [13–17]. Many of these domains are believed to be important for the maintenance of membrane structure and function. In addition, cholesterol is known to increase the thickness of the lipid bilayer [18], and modulate the dielectric property of the membrane interior by altering water permeation characteristics [19]. In this paper, we have monitored the organization and dynamics of Nile Red in membranes containing various amounts of cholesterol utilizing sensitive fluorescence techniques which include the red edge excitation shift (REES) approach. In addition, we have analyzed the depth of penetration of Nile Red in membranes using the parallax method [20].
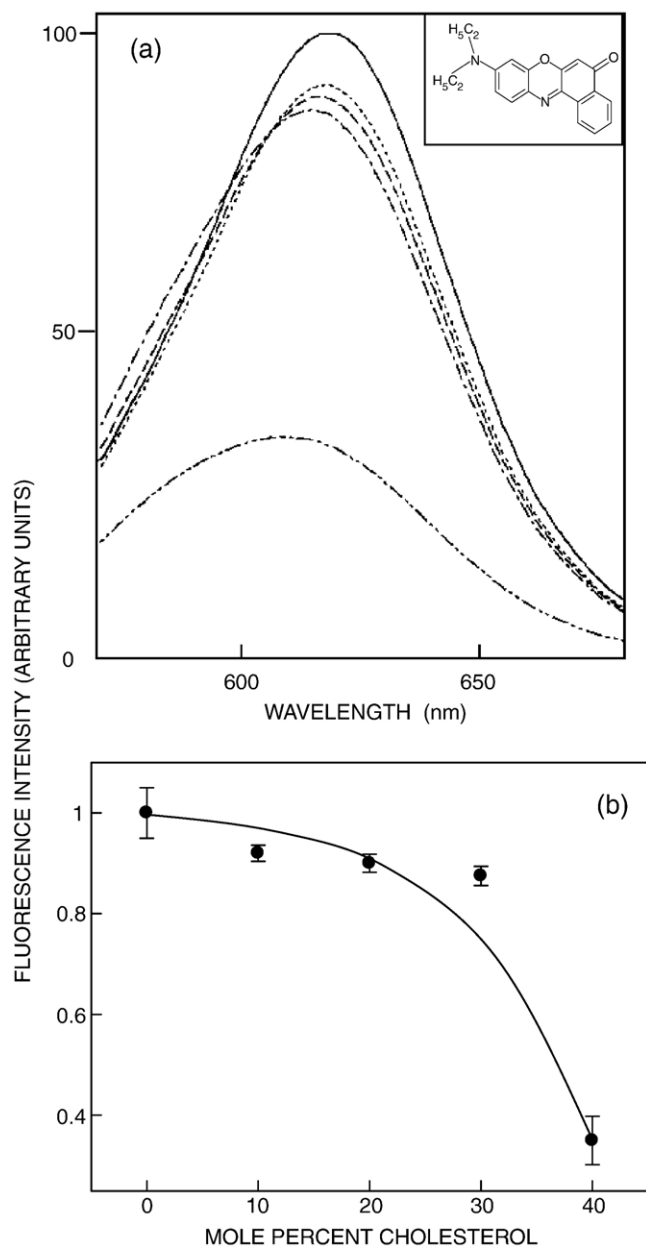
Fig. 1. Effect of increasing amounts of cholesterol on fluorescence emission spectra and fluorescence intensity of Nile Red in DOPC vesicles: (a) representative fluorescence spectra of Nile Red in DOPC vesicles containing 0 (⎯), 10 (−−−−), 20 (__ __), 30 (· ⎯ ·) and 40 (__ − −) mol% cholesterol; and (b) fluorescence intensity of Nile Red in DOPC vesicles as a function of increasing cholesterol concentration. Fluorescence intensity was monitored at the respective emission maximum in case of each sample and the excitation wavelength was kept at 550 nm. The data points shown are the means±S.E. of three independent measurements. The ratio of Nile Red to total lipid was 1:100 (mol/mol) and the concentration of Nile Red was 1.6 μM in all cases. See Materials and methods for other details. The inset in panel a shows the chemical structure of Nile Red.

2. Materials and methods

2.1. Materials

DOPC, Tempo-PC, and 5-PC were obtained from Avanti Polar Lipids (Alabaster, AL). 2- and 12-AS were from Molecular Probes (Eugene, OR). Cholesterol, DMPC, Na_2HPO_4, Nile Red and MOPS were obtained from Sigma

Chemical Co. (St. Louis, MO). Lipids were checked for purity by thin layer chromatography on silica gel precoated plates (Sigma) in chloroform/methanol/water (65:35:5, v/v/v), and were found to give only one spot in all cases with a phosphate-sensitive spray and on subsequent charring [21]. The concentration of stock solution of DOPC was determined by phosphate assay subsequent to total digestion by perchloric acid [22]. DMPC was used as an internal standard to assess lipid digestion. Cholesterol was estimated using the Amplex Red cholesterol assay kit [23]. Concentration of stock solution of Nile Red in methanol was estimated using its molar extinction coefficients (ε) of 45,000 M^{-1} cm^{-1} at 552 nm [24]. All other chemicals used were of the highest purity available. Solvents used were of spectroscopic grade. Water was purified through a Millipore (Bedford, MA) Milli-Q system and used throughout.

2.2. Methods

2.2.1. Sample preparation

All experiments were done using large unilamellar vesicles (LUVs) of 100 nm diameter of DOPC containing increasing concentrations (0–40 mol%) of cholesterol and 1 mol% Nile Red. In general, 320 nmol (1280 nmol for time-resolved fluorescence measurements) of total lipid (DOPC or DOPC/cholesterol) in methanol was mixed with 3.2 nmol (12.8 nmol for time-resolved fluorescence measurements) of Nile Red in methanol. The sample was mixed well and dried under a stream of nitrogen while being warmed gently (∼35 °C). After further drying under a high vacuum for at least 6 h, 1.5 ml of 10 mM MOPS, 150 mM sodium chloride, pH 7.4 buffer was added, and the samples were vortexed for 3 min to disperse the lipid and form homogeneous multilamellar vesicles. LUVs of diameter of 100 nm were prepared by the extrusion technique using an Avestin Liposofast Extruder (Ottawa, Ontario, Canada) as previously described [17]. In order to ensure that no loss of cholesterol took place during extrusion, we estimated the phospholipid and cholesterol contents of the vesicles before and after extrusion using phosphate [22] and cholesterol [23] assays. The cholesterol content of the extruded vesicles was found to be within 2% of the expected value. Samples were incubated in dark for 12 h at room temperature (∼23 °C) for equilibration before measuring fluorescence. Background samples were prepared in the same way except that Nile Red was not added to them.

2.2.2. Depth measurements using the parallax method

The actual spin (nitroxide) content of the spin-labeled phospholipids (Tempo- and 5-PC) was assayed using fluorescence quenching of anthroyloxy-labeled fatty acids (2- and 12-AS) as described earlier [25]. For depth measurements, multilamellar vesicles were made by co-drying 160 nmol of total lipid (DOPC or DOPC/cholesterol) containing 10 mol% spin-labeled phospholipid (Tempo- and 5-PC) and Nile Red (1 mol%) under a stream of nitrogen while being warmed gently (∼35 °C) followed by further drying under high vacuum for 3 h. The dried lipid film was hydrated with 1.5 ml of 10 mM MOPS, 150 mM sodium chloride, pH 7.4 buffer. Duplicate samples were prepared in each case except for samples lacking the quencher (Tempo- and 5-PC) for which triplicates were prepared. Background samples lacking Nile Red were prepared in all cases, and their fluorescence intensity was subtracted from the respective sample fluorescence intensity. Samples were kept in dark for 12 h before measuring fluorescence.

2.2.3. Steady state fluorescence measurements

Steady state fluorescence measurements were performed with a Hitachi F-4010 spectrofluorometer using 1 cm path length quartz cuvettes. Excitation and emission slits with a nominal bandpass of 5 nm were used for all measurements. Background intensities of samples in which Nile Red was omitted were negligible in most cases and were subtracted from each sample spectrum to cancel out any contribution due to the solvent Raman peak and other scattering artifacts. The spectral shifts obtained with different sets of samples were identical in most cases. In other cases, the values were within ± 1 nm of the ones reported. Fluorescence polarization measurements were performed using a Hitachi polarization accessory. Polarization values were calculated from the equation [26]:

$$P = \frac{I_{VV} - G I_{VH}}{I_{VV} + G I_{VH}} \tag{1}$$

where I_{VV} and I_{VH} are the measured fluorescence intensities (after appropriate background subtraction) with the excitation polarizer vertically oriented and emission polarizer vertically and horizontally oriented, respectively. G is the grating correction factor and is the ratio of the efficiencies of the detection system for vertically and horizontally polarized light, and is equal to I_{HV}/I_{HH}. All experiments were done with multiple sets of samples and average values of polarization are shown in Fig. 3.

For depth measurements, samples were excited at 553 nm and emission was collected at 618 nm. Excitation and emission slits with nominal bandpass of 5 nm were used. Fluorescence was measured at room temperature (∼23 °C) and averaged over two 5-s readings. Samples were kept in dark for 30 sec in the fluorimeter between two readings to avoid any photodamage. Intensities were found to be stable over time. In all cases, intensities from background samples (without fluorophore) were subtracted. Membrane penetration depths were calculated using Eq. (4) (see Results).

2.2.4. Time-resolved fluorescence measurements

Fluorescence lifetimes were calculated from time-resolved fluorescence intensity decays using a Photon Technology International (London, Western Ontario, Canada) LS-100 luminescence spectrophotometer in the time-correlated single photon counting mode using 1 cm path length quartz cuvettes. This machine uses a thyratron-gated nanosecond flash lamp filled with nitrogen as the plasma gas (16±1 in. of mercury vacuum) and is run at 17–22 kHz. Lamp profiles were measured at the excitation wavelength using Ludox (colloidal silica) as the scatterer. To optimize the signal to noise ratio, 10,000 photon counts were collected in the peak channel. The excitation wavelength used was 553 nm and the emission wavelength was set at 610 nm. All experiments were performed using excitation and emission slits with bandpass of 8 nm or less. The sample and the scatterer were alternated after every 5% acquisition (i.e., after 500 counts are collected in the peak channel each time) to ensure compensation for shape and timing drifts occurring during the period of data collection. This arrangement also prevents any prolonged exposure of the sample to the excitation beam thereby avoiding any possible photodamage of the fluorophore. The data stored in a multichannel analyzer was routinely transferred to an IBM PC for analysis. Fluorescence intensity decay curves so obtained were deconvoluted with the instrument response function and analyzed as a sum of exponential terms:

$$F(t) = \Sigma_i \alpha_i \exp(-t/\tau_i) \qquad (2)$$

where $F(t)$ is the fluorescence intensity at time t and α_i is a preexponential factor representing the fractional contribution to the time-resolved decay of the component with a lifetime τ_i such that $\Sigma_i \, \alpha_i = 1$. The decay parameters were recovered using a nonlinear least squares iterative fitting procedure based on the Marquardt algorithm [27]. The program also includes statistical and plotting subroutine packages [28]. The goodness of the fit of a given set of observed data and the chosen function was evaluated by the reduced χ^2 ratio, the weighted residuals [29], and the autocorrelation function of the weighted residuals [30]. A fit was considered acceptable when plots of the weighted residuals and the autocorrelation function showed random deviation about zero with a minimum χ^2 value not more than 1.4. Mean (average) lifetimes $\langle\tau\rangle$ for biexponential decays of fluorescence were calculated from the decay times and preexponential factors using the following equation [26]:

$$\langle\tau\rangle = \frac{\alpha_1 \tau_1^2 + \alpha_2 \tau_2^2}{\alpha_1 \tau_1 + \alpha_2 \tau_2} \qquad (3)$$

3. Results

3.1. Fluorescence characteristics of Nile Red in DOPC vesicles containing cholesterol

The fluorescence of Nile Red is known to be sensitive to the polarity of the medium, i.e., the dielectric environment. In a polar environment, Nile Red has a low fluorescence quantum yield, whereas in more hydrophobic environments its quantum

Table 1
Fluorescence lifetimes [a] of Nile Red in DOPC vesicles with increasing cholesterol concentration

Cholesterol (mol%)	α_1	τ_1 (ns)	α_2	τ_2 (ns)
0	0.25	4.66	0.75	2.88
10	0.34	3.80	0.66	3.34
20	0.28	3.72	0.72	3.51
30	0.17	3.92	0.83	3.77
40	0.28	4.10	0.72	3.62

[a] The excitation wavelength was 553 nm and emission was monitored at 610 nm. The ratio of Nile Red/total lipid was 1:100 (mol/mol) and the concentration of Nile Red was 6.4 μM.

yield increases and its emission maximum becomes progressively blue shifted [2–5]. The fluorescence emission spectra of Nile Red in DOPC vesicles with increasing cholesterol concentration are shown in Fig. 1a. The emission maximum[1] of Nile Red in DOPC vesicles in the absence of cholesterol is found to be 616 nm when excited at 530 nm. The emission maximum displays progressive blue shift toward lower wavelength with increasing cholesterol concentration, and reaches a value of 605 nm in the presence of 40 mol% cholesterol. This blue shift in emission maximum in presence of cholesterol could possibly indicate a deeper localization of Nile Red in cholesterol-containing membranes, as evident from analysis of membrane penetration depth (see Table 2). Interestingly, the blue shift in emission maximum of Nile Red with increasing cholesterol is accompanied with a reduction in fluorescence intensity (see Fig. 1b). While this is somewhat surprising, it brings out the fact that the fluorescence emission maximum is influenced by a number of environmental factors and it is not always easy to interpret peak shifts in emission maximum, especially in a microheterogeneous medium such as membranes. The peak fluorescence intensity drops by ∼65% when cholesterol concentration is increased to 40 mol%, possibly due to induction of the liquid-ordered-like phase (see later). The reduction in fluorescence intensity with increasing cholesterol concentration could be due to an increase in environmental polarity due to increased water penetration in the membrane interfacial region (where Nile Red is localized, see later) induced by cholesterol [31].

3.2. Red edge excitation shift and fluorescence polarization of Nile Red in DOPC vesicles containing cholesterol

Red edge excitation shift (REES) represents a powerful approach which can be used to directly monitor the environment and dynamics around a fluorophore in a complex biological system [32,33]. A shift in the wavelength of maximum fluorescence emission toward higher wavelengths, caused by a shift

---

[1] We have used the term maximum of fluorescence emission in a somewhat wider sense here. In every case, we have monitored the wavelength corresponding to maximum fluorescence intensity, as well as the center of mass of the fluorescence emission. In most cases, both these methods yielded the same wavelength. In cases where minor discrepancies were found, the center of mass of emission has been reported as the fluorescence maximum.

in the excitation wavelength toward the red edge of absorption band, is termed REES. This effect is mostly observed with polar fluorophores in motionally restricted environments such as viscous solutions or condensed phases where the dipolar relaxation time for the solvent shell around a fluorophore is comparable to or longer than its fluorescence lifetime [32–34]. REES arises due to slow rates of solvent relaxation (reorientation) around an excited state fluorophore, which is dependent on the motional restriction imposed on the solvent molecules in the immediate vicinity of the fluorophore. Utilizing this approach, it becomes possible to probe the mobility parameters of the environment itself (represented by the relaxing solvent molecules) using the fluorophore merely as a reporter group. Further, since the ubiquitous solvent for biological systems is water, the information obtained in such cases will come from the otherwise 'optically silent' water molecules. The unique feature of REES is that while other fluorescence techniques yield information about the fluorophore itself, REES provides information about the relative rates of solvent relaxation which is not possible to obtain by other techniques. This makes REES extremely useful since hydration plays a crucial modulatory role in a large number of important cellular events such as protein folding, lipid–protein interactions and ion transport [35].

The shifts in the maxima of fluorescence emission of Nile Red in DOPC vesicles with increasing concentration of cholesterol as a function of excitation wavelength are shown in Fig. 2a. As the excitation wavelength is changed from 530 to 600 nm, the emission maxima of Nile Red display shifts toward longer wavelengths in all cases. The emission maxima are shifted from 616 to 623 nm (in the absence of cholesterol), 613 to 622 nm (20 mol% cholesterol), 611 to 622 nm (30 mol% cholesterol), and 605 to 622 nm (40 mol% cholesterol) which correspond to REES of 7–17 nm in these cases. Such dependence of the emission spectra on the excitation wavelength is characteristic of the red edge effect. Observation of REES in DOPC vesicles implies that Nile Red is in a motionally restricted environment in the membrane, possibly at the membrane interface (see later). The observed red edge effect would directly imply that the region of the membrane, where Nile Red is localized, offers considerable restriction to the reorientational motion of the solvent dipoles around the excited state fluorophore.

The magnitude of REES of Nile Red in DOPC vesicles with increasing cholesterol content (from Fig. 2a) is shown in Fig. 2b. As is apparent from the figure, the extent of REES is found to increase with increasing concentration of cholesterol indicating an increase in the overall motional restriction experienced by the reorienting solvent molecules. This means that there is a change in the microenvironment of Nile Red in DOPC vesicles with increasing cholesterol content.

In addition to the dependence of fluorescence emission maxima on the excitation wavelength, fluorescence polarization is also known to depend on the excitation wavelength in motionally restricted media [36]. Due to strong dipolar interactions with the surrounding solvent molecules, there is a decreased rotational rate of the fluorophore in the relaxed state.

On red edge excitation, a selective excitation of this subclass of fluorophores occurs. Because of strong interaction with the polar solvent molecules with this subclass of fluorophores in the excited state, one may expect these "solvent relaxed" fluorophores to rotate more slowly, thereby increasing the polarization. The excitation polarization spectra (*i.e.*, a plot of steady state polarization *vs.* excitation wavelength) of Nile Red in DOPC vesicles containing varying amounts of cholesterol are shown in Fig. 3a. Interestingly, the polarization of Nile Red in these membranes shows considerable increase upon increasing the excitation wavelength from 530 to 600 nm (Fig. 3a). Such an increase in polarization upon red edge excitation has been previously reported for fluorophores in motionally restricted media [36].

Fig. 3b shows the variation in steady state polarization of Nile Red in DOPC vesicles containing cholesterol as a function of wavelength across its emission spectrum. As seen
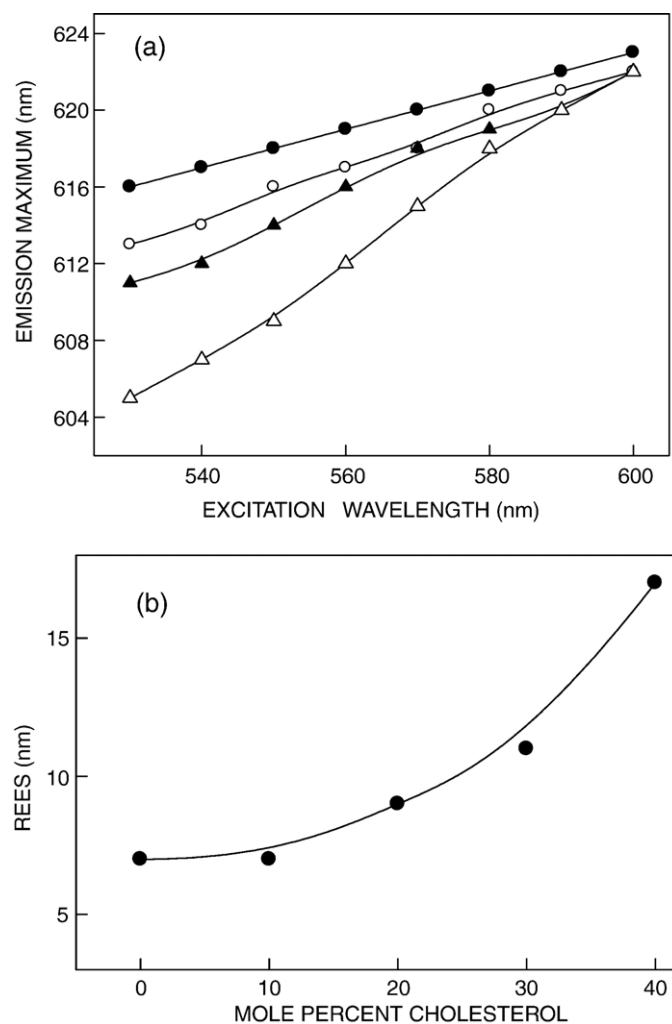

Fig. 2. (a) Effect of changing excitation wavelength on the wavelength of maximum emission of Nile Red in DOPC vesicles containing 0 (●), 20 (○), 30 (▲) and 40 (△) mol% cholesterol. (b) Effect of increasing amounts of cholesterol on the magnitude of red edge excitation shift (REES) of Nile Red in DOPC vesicles. REES data obtained from (a) are plotted as a function of increasing cholesterol concentration. All other conditions are as in Fig. 1. See Materials and methods for other details.

from the figure, there is a considerable decrease in polarization with increasing emission wavelength in all the cases. The lowest polarization is observed toward longer wavelengths (red

edge) where emission from the relaxed fluorophores predominates. Similar observations have previously been reported for other fluorophores in environments of restricted mobility [36]. This provides further support to our earlier REES results reinforcing that Nile Red is localized in a motionally restricted region of the membrane in these cases.

The steady state polarization of Nile Red in DOPC vesicles as a function of increasing concentration of cholesterol is shown in Fig. 3c. Interestingly, the fluorescence polarization of Nile Red shows an initial decrease (up to ∼20 mol%) and then gradually increases till 40 mol% cholesterol. The initial decrease in polarization could indicate a possible decrease in membrane order around Nile Red. The increase in polarization beyond 20 mol% cholesterol, could possibly be attributed to the recently reported liquid-ordered-like phase formed in DOPC membranes containing high amount of cholesterol [37]. Interestingly, it is not absolutely clear what is the threshold concentration of cholesterol needed to induce the liquid-ordered phase. While it has been reported that the liquid-ordered-like phase can be detected at 30 mol% cholesterol in a DOPC-cholesterol membrane system [37], a precise concentration dependence of this phase is lacking.
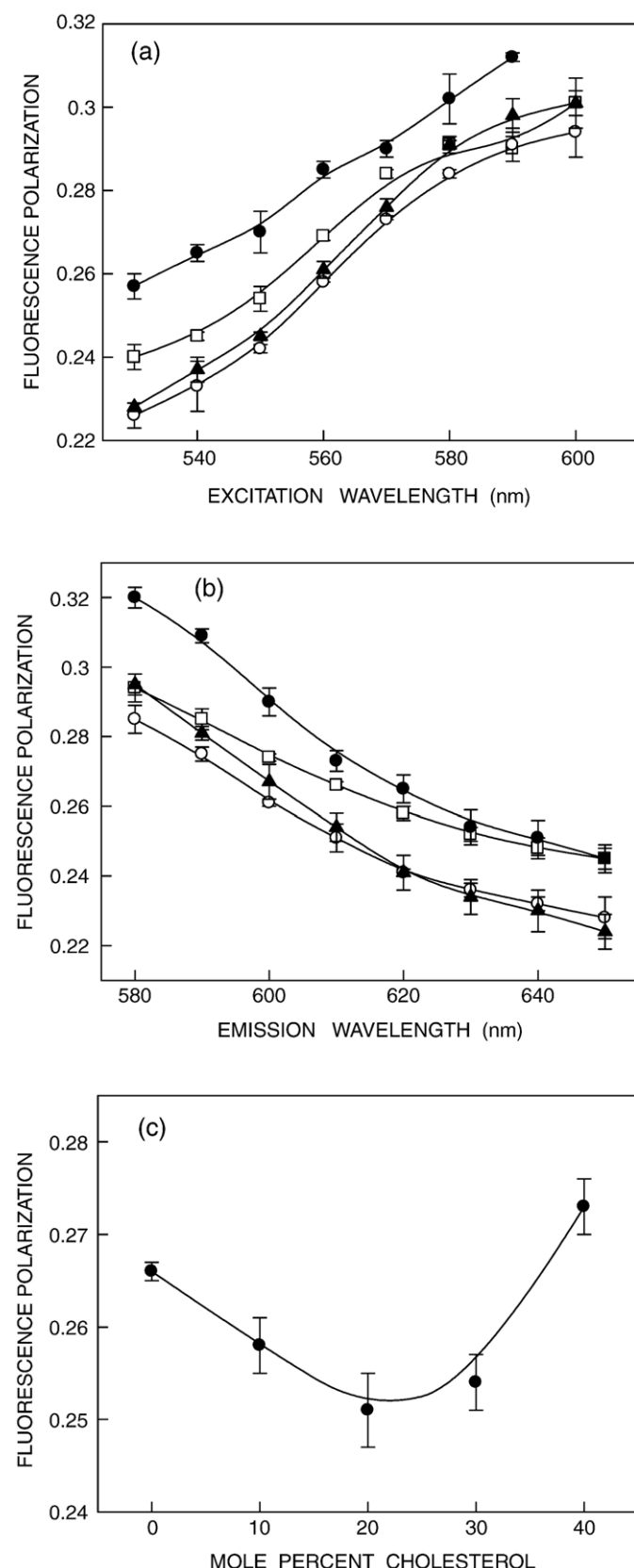
3.3. Time-resolved fluorescence measurements of Nile Red in DOPC vesicles containing cholesterol

Fluorescence lifetime serves as a faithful indicator of the local environment in which a given fluorophore is placed. In addition, it is well known that fluorescence lifetime of Nile Red is sensitive to solvent properties, temperature and excited state interactions [3–5]. A typical intensity decay profile of Nile Red in DOPC vesicles with its biexponential fitting and the various statistical parameters used to check the goodness of the fit is shown in Fig. 4. Table 1 shows the lifetimes of Nile Red in DOPC vesicles as a function of increasing concentration of cholesterol. All fluorescence decays for membrane bound Nile Red obtained could be fitted well with a biexponential function. We chose to use the mean fluorescence lifetime as an important parameter for describing the behavior of Nile Red in DOPC membranes since it is independent of the method of analysis and the number of exponentials used to fit the time-resolved fluorescence decay. The mean fluorescence lifetimes of Nile Red in DOPC and DOPC/cholesterol membranes were calculated from Table 1 using Eq. (3) and are plotted as a function of increasing

Fig. 3. Fluorescence polarization of Nile Red in DOPC vesicles containing 0 (□), 20 (○), 30 (▲) and 40 (●) mol% cholesterol as a function of (a) excitation wavelength (the emission wavelength was set at the respective emission maximum in each case), and (b) emission wavelength (the excitation wavelength was kept at 553 nm in all cases). The data points shown are the means±S.E. of three independent measurements. (c) Change in fluorescence polarization of Nile Red in DOPC vesicles as a function of increasing concentration of cholesterol. The excitation wavelength was 553 nm and emission was monitored at 610 nm. All other conditions are as in Fig. 1. See Materials and methods for other details.
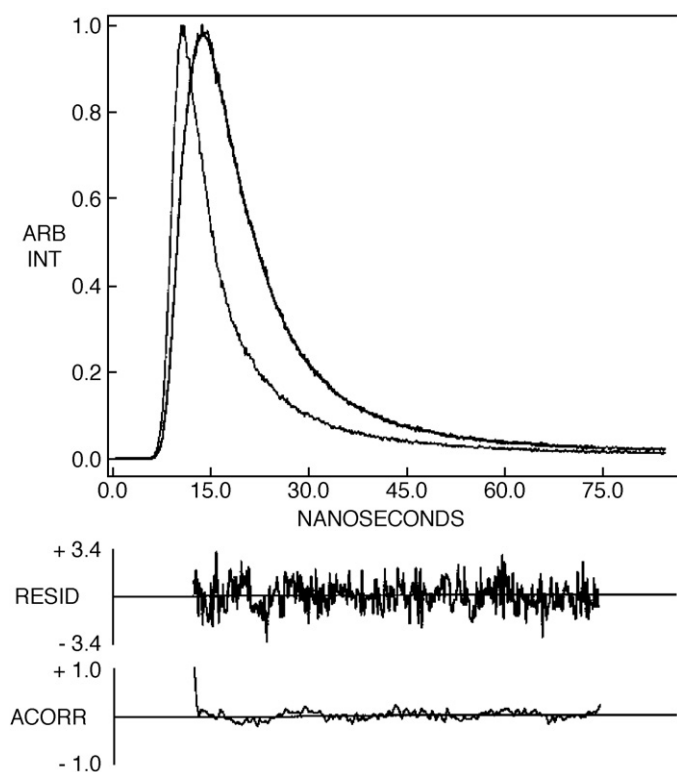
Fig. 4. Time-resolved fluorescence intensity decay of Nile Red in DOPC vesicles. The excitation wavelength was 553 nm and emission was monitored at 610 nm. The sharp peak on the left is the lamp profile. The relatively broad peak on the right is the decay profile, fitted to a biexponential function. The two lower plots show the weighted residuals and the autocorrelation function of the weighted residuals. The ratio of Nile Red to total lipid was 1:100 (mol/mol) and the concentration of Nile Red was 6.4 μM. All other conditions are as in Fig. 1. See Materials and methods for other details.
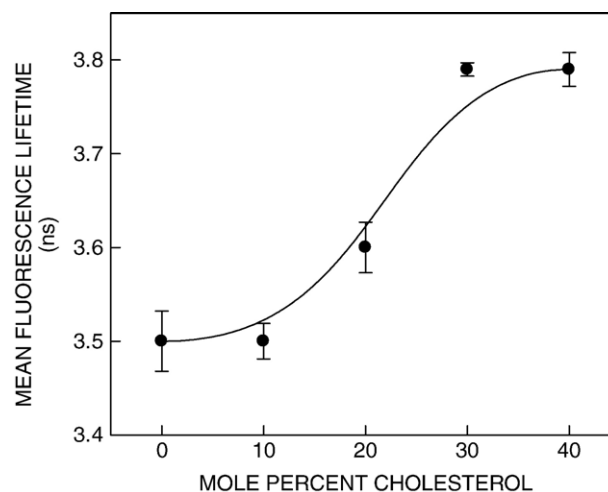

Fig. 5. Effect of increasing amounts of cholesterol on mean fluorescence lifetime of Nile Red in DOPC vesicles. Samples were excited at 553 nm while emission was monitored at 610 nm. Mean fluorescence lifetimes were calculated from Table 1 using Eq. (3). All other conditions are as in Fig. 4. See Materials and methods for other details.

concentration of cholesterol in Fig. 5. There is a small (∼9%) increase in mean fluorescence lifetime of Nile Red from ∼3.5 to 3.8 ns with increase in membrane cholesterol content up to 40 mol%. The increase in Nile Red lifetime in membranes containing high amount of cholesterol could possibly indicate the presence of liquid-ordered-like phase, as mentioned earlier [37].

Table 2
Membrane penetration depth of Nile Red in DOPC vesicles with increasing cholesterol concentration by the parallax method

Cholesterol [a] (mol%)	Distance from the center of the bilayer z_{cF} (Å) [b]
0	17.6
20	16.6
40	15.8

[a] Corrections were made for the altered concentrations of spin-labeled lipids (for lateral distribution) and the depths of the quenchers used in membranes containing cholesterol [40].
[b] Depths were calculated from fluorescence quenchings obtained with samples containing 10 mol% of Tempo-PC and 5-PC and using Eq. (4). Samples were excited at 553 nm, and emission was collected at 618 nm. The ratio of Nile Red/total lipid was 1:100 (mol/mol) and the concentration of Nile Red was 1.07 μM in all cases. See Materials and methods for other details.

3.4. Cholesterol influences the depth of Nile Red in DOPC vesicles containing cholesterol

Membrane penetration depth represents an important parameter in the study of membrane structure and organization [38,39]. Knowledge of the precise depth of a membrane-embedded group or molecule often helps define the conformation and topology of membrane probes and proteins. In addition, properties such as polarity, fluidity, segmental motion, ability to form hydrogen bonds and the extent of solvent penetration are known to vary in a depth dependent manner in the membrane. To gain a better understanding of the location of Nile Red in DOPC membranes containing varying amounts of cholesterol, penetration depths of Nile Red in membranes were determined. Depth of Nile Red was calculated by the parallax method [20] using the equation:

$$z_{cF} = L_{c1} + \{[(-1/\pi C)\ln(F_1/F_2) - L_{21}^2]/2\, L_{21}\} \qquad (4)$$

where z_{cF} = the depth of the fluorophore from the center of the bilayer, L_{c1} = the distance of the center of the bilayer from the shallow quencher (Tempo-PC in this case), L_{21} = the difference in depth between the two quenchers (i.e., the transverse distance between the shallow and the deep quencher), and C = the two-dimensional quencher concentration in the plane of the membrane (molecules/Å^2). Here F_1/F_2 is the ratio of F_1/F_o and F_2/F_o in which F_1 and F_2 are fluorescence intensities in the presence of the shallow (Tempo-PC) and deep quencher (5-PC), respectively, both at the same quencher concentration C; F_o is the fluorescence intensity in the absence of any quencher. All the bilayer parameters used were the same as described previously [20]. The depths of penetration of Nile Red in DOPC vesicles containing cholesterol are shown in Table 2.

Table 2 shows that Nile Red is localized at a distance of 17.6 Å from the center of the bilayer (see Fig. 6). This suggests
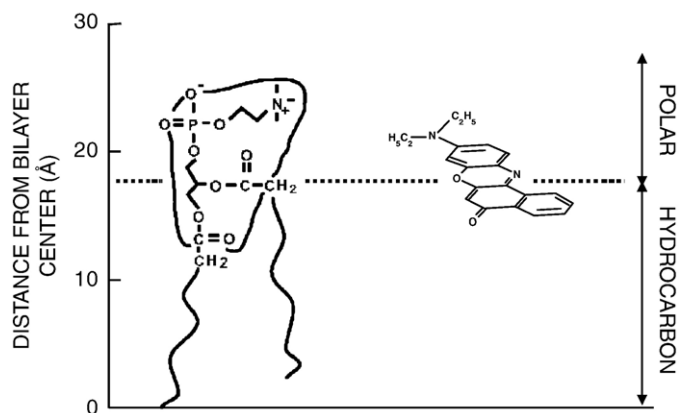
Fig. 6. A schematic representation of half of the membrane bilayer showing the localization of Nile Red in phosphatidylcholine membranes. The horizontal line at the bottom indicates the center of the bilayer.

that Nile Red is localized at the interfacial region of the membrane. Interestingly, the depth of penetration of Nile Red changes to 16.6 and 15.8 Å in DOPC vesicles containing 20 and 40 mol% cholesterol, respectively (see Table 2). This indicates that Nile Red is localized at a relatively deeper interfacial region in membranes containing cholesterol (see Table 2). This observation is consistent with the relatively blue-shifted fluorescence emission maximum of Nile Red in DOPC membranes in the presence of cholesterol. Taken together, these results suggest that the environment and location experienced by Nile Red could depend on the cholesterol content in the membrane.

4. Discussion

Although Nile Red has previously been used to monitor membrane organization and heterogeneity [8,11,12], properties of Nile Red when incorporated in membranes including its localization in the membrane is not yet explored. In this paper, we have monitored the organization and dynamics of Nile Red incorporated in DOPC vesicles containing varying amounts of cholesterol utilizing fluorescence-based approaches which include the REES approach and the parallax method for depth determination. Our results show that the fluorescence emission maximum, intensity, polarization, and lifetime of Nile Red is dependent on the cholesterol content in the membrane. Interestingly, Nile Red exhibits significant REES independent of the presence of cholesterol. This indicates that Nile Red is localized in a motionally restricted environment in the membrane (see later).

An important criterion for a fluorophore to be able to exhibit REES is that it should be polar, that is, it should have a permanent dipole moment in the ground state. In addition, there should be a significant change in the dipole moment upon excitation, so as to cause the solvent dipoles to reorient in response to this altered dipole moment in order to attain an energetically favorable orientation [32,36]. For a totally nonpolar fluorophore, there will be no change in dipole moment upon excitation, and the process of solvent reorientation

becomes irrelevant, since it is the change in dipole moment that triggers the solvent reorientation. It has been previously shown that the dipole moment of Nile Red changes by ∼7–10 D upon excitation [3–5]. A change in dipole moment of this magnitude, along with its hydrogen bonding capability makes Nile Red a suitable probe for REES effects in order to characterize the hydrophobic binding sites in proteins and membranes.

Importantly, analysis of membrane penetration depth using the parallax method points out to an interfacial localization of Nile Red in membranes although it is predominantly a hydrophobic molecule. The interfacial region of the membrane is characterized by unique motional and dielectric characteristics different from the bulk aqueous phase and the more isotropic hydrocarbon-like deeper regions of the membrane and plays an important role in functional aspects such as substrate recognition and activity of lipolytic enzymes [32]. This specific region of the membrane exhibits slow rates of solvent relaxation and is also known to participate in intermolecular charge interactions and hydrogen bonding through the polar head-group. These structural features which slow down the rate of solvent reorientation have previously been recognized as typical features of solvents giving rise to significant red edge effects [32]. It is therefore the membrane interface which is most likely to display red edge effects and is sensitive to wavelength-selective fluorescence measurements.

Work from a number of laboratories have shown that aromatic molecules (molecules containing delocalized electrons) tend to be localized at the membrane interface. For example, it is becoming increasingly evident that tryptophan residues in integral membrane proteins and peptides are not uniformly distributed and that they tend to be localized toward the membrane interface, possibly because they are involved in hydrogen bonding [33,41]. In addition, the aromatic fluorescent hydrocarbon pyrene has recently been shown to be localized in the interfacial region of the membrane [42]. In this context, the interfacial localization of Nile Red in the membrane is logical.

Taken together, our results show that the hydrophobic fluorescent probe Nile Red is localized at the membrane interface. In addition, the environment and location experienced by Nile Red depend on the cholesterol content of the membrane. These results could be useful in future studies involving Nile Red in characterizing cholesterol-induced membrane heterogeneity in complex biological membranes such as neuronal membranes.

References

[1] A. Chattopadhyay (Ed.), Lipid probes in membrane biology, Chem. Phys. Lipids, vol. 116, 2002, pp. 1–194.

[2] P. Greenspan, S.D. Fowler, Spectrofluorometric studies of the lipid probe, Nile Red, J. Lipid Res. 26 (1985) 781–789.

[3] A.K. Dutta, K. Kamada, K. Ohta, Spectroscopic studies of Nile Red in organic solvents and polymers, J. Photochem. Photobiol., A Chem. 93 (1996) 57–64.

[4] N. Ghoneim, Photophysics of Nile Red in solution steady state spectroscopy, Spectrochim. Acta A 56 (2000) 1003–1010.

[5] C.M. Golini, B.W. Williams, J.B. Foresman, Further solvatochromic, thermochromic, and theoretical studies on Nile Red, J. Fluoresc. 8 (1998) 395–404.

[6] D.L. Sackett, J.R. Knutson, J. Wolff, Hydrophobic surfaces of tubulin probed by time-resolved and steady-state fluorescence of Nile Red, J. Biol. Chem. 265 (1990) 14899–14906.

[7] J.-R. Daban, M. Samsó, S. Bartolomé, Use of Nile Red as a fluorescent probe for the study of the hydrophobic properties of protein–sodium dodecyl complexes in solution, Anal. Biochem. 199 (1991) 162–168.

[8] F. Gao, E. Mei, M. Lim, R.M. Hochstrasser, Probing lipid vesicles by bimolecular association and dissociation trajectories of single molecules, J. Am. Chem. Soc. 128 (2006) 4814–4822.

[9] N.A. Pham, M.R. Gal, R.D. Bagshaw, A.J. Mohr, B. Chue, T. Richardson, J.W. Callahan, A comparative study of cytoplasmic granules imaged by the real-time microscope, Nile Red and Filipin in fibroblasts from patients with lipid storage diseases, J. Inherit. Metab. Dis. 28 (2005) 991–1004.

[10] E. Kahn, A. Vejux, D. Dumas, T. Montange, F. Frouin, V. Robert, J.M. Riedinger, J.F. Stoltz, P. Gambert, A. Todd-Pokropek, G. Lizard, FRET multiphoton spectral imaging microscopy of 7-ketocholesterol and Nile Red in U937 monocytic cells loaded with 7-ketocholesterol, Anal. Quant. Cytol. Histol. 26 (2004) 304–313.

[11] G. Krishnamoorthy, Ira, Fluorescence lifetime distribution in characterizing membrane heterogeneity, J. Fluoresc. 11 (2001) 247–253.

[12] Ira, G. Krishnamoorthy, Probing the link between proton transport and water content in lipid membranes, J. Phys. Chem., B 105 (2001) 1484–1488.

[13] L. Liscum, K.W. Underwood, Intracellular cholesterol transport and compartmentation, J. Biol. Chem. 270 (1995) 15443–15446.

[14] K. Simons, E. Ikonen, How cells handle cholesterol, Science 290 (2000) 1721–1725.

[15] K. Simons, E. Ikonen, Functional rafts in cell membranes, Nature 387 (1997) 569–572.

[16] X. Xu, E. London, The effect of sterol structure on membrane lipid domains reveals how cholesterol can induce lipid domain formation, Biochemistry 39 (2000) 843–849.

[17] R. Rukmini, S.S. Rawat, S.C. Biswas, A. Chattopadhyay, Cholesterol organization in membranes at low concentrations: effects of curvature stress and membrane thickness, Biophys. J. 81 (2001) 2122–2134.

[18] F.A. Nezil, M. Bloom, Combined influence of cholesterol and synthetic amphiphilic peptides upon bilayer thickness in model membranes, Biophys. J. 61 (1992) 1176–1183.

[19] S.A. Simon, T.J. McIntosh, R. Latorre, Influence of cholesterol on water penetration into bilayers, Science 216 (1982) 65–67.

[20] A. Chattopadhyay, E. London, Parallax method for direct measurement of membrane penetration depth utilizing fluorescence quenching by spin-labeled phospholipids, Biochemistry 26 (1987) 39–45.

[21] J.C. Dittmer, R.L. Lester, A simple, specific spray for the detection of phospholipids on thin-layer chromatograms, J. Lipid Res. 5 (1964) 126–127.

[22] C.W.F. McClare, An accurate and convenient organic phosphorus assay, Anal. Biochem. 39 (1971) 527–530.

[23] D.M. Amundson, M. Zhou, Fluorometric method for the enzymatic determination of cholesterol, J. Biochem. Biophys. Methods 38 (1999) 43–52.

[24] R.P. Haugland, Handbook of Fluorescent Probes and Research Chemicals, 6th Ed. Molecular Probes Inc., Eugene, OR, USA, 1996.

[25] F.S. Abrams, E. London, Extension of the parallax analysis of membrane penetration depth to the polar region of model membranes: use of fluorescence quenching by a spin-label attached to the phospholipid polar headgroup, Biochemistry 32 (1993) 10826–10831.

[26] J.R. Lakowicz, Principles of Fluorescence Spectroscopy, Kluwer-Plenum Press, New York, 1999.

[27] P.R. Bevington, Data Reduction and Error Analysis for the Physical Sciences, McGraw-Hill, New York, 1969.

[28] D.V. O'Connor, D. Phillips, Time-Correlated Single Photon Counting, Academic Press, London, 1984, pp. 180–189.

[29] R.A. Lampert, L.A. Chewter, D. Phillips, D.V. O'Connor, A.J. Roberts, S. R. Meech, Standards for nanosecond fluorescence decay time measurements, Anal. Chem. 55 (1983) 68–73.

[30] A. Grinvald, I.Z. Steinberg, On the analysis of fluorescence decay kinetics by the method of least-squares, Anal. Biochem. 59 (1974) 583–598.

[31] W.K. Subczynski, A. Wisniewska, J.-J. Yin, J.S. Hyde, A. Kusumi, Hydrophobic barriers of lipid bilayer membranes formed by reduction of water penetration by alkyl chain unsaturation and cholesterol, Biochemistry 33 (1994) 7670–7681.

[32] A. Chattopadhyay, Exploring membrane organization and dynamics by the wavelength-selective fluorescence approach, Chem. Phys. Lipids 122 (2003) 3–17.

[33] H. Raghuraman, D.A. Kelkar, A. Chattopadhyay, Novel insights into proteinstructure and dynamics utilizing the red edge excitation shift approach, in: C.D. Geddes, J.R. Lakowicz (Eds.), Reviews in Fluorescence, Springer, New York, 2005, pp. 199–214.

[34] A.P. Demchenko, The red-edge effects: 30 years of exploration, Luminescence 17 (2002) 19–42.

[35] P. Mentré (Ed.), Water in the Cell, Cell. Mol. Biol., vol. 47, 2001, pp. 709–970.

[36] S. Mukherjee, A. Chattopadhyay, Wavelength-selective fluorescence as a novel tool to study organization and dynamics in complex biological systems, J. Fluoresc. 5 (1995) 237–246.

[37] D.E. Warschawski, P.E. Devaux, Order parameters of unsaturated phospholipids in membranes and the effect of cholesterol: a ^{1}H–^{13}C solid-state NMR study at natural abundance, Eur. Biophys. J. 34 (2005) 987–996.

[38] A. Chattopadhyay, Membrane penetration depth analysis using fluorescence quenching: a critical review, in: B.P. Gaber, K.R.K. Easwaran (Eds.), Biomembrane Structure and Function: The State of the Art, Adenine Press, Schenectady, NY, 1992, pp. 153–163.

[39] E. London, A.S. Ladokhin, Measuring the depth of amino acid residues in membrane-inserted peptides by fluorescence quenching, in: D. Benos, S. Simon (Eds.), Current Topics in Membranes, vol. 52, Elsevier, San Diego, 2002, pp. 89–115.

[40] R.D. Kaiser, E. London, Location of diphenylhexatriene (DPH) and its derivatives within membranes: comparison of different fluorescence quenching analyses of membrane depth, Biochemistry 37 (1998) 8180–8190.

[41] W.-M. Yau, W.C. Wimley, K. Gawrisch, S.H. White, The preference of tryptophan for membrane interfaces, Biochemistry 37 (1998) 14713–14718.

[42] B. Hoff, E. Strandberg, A.S. Ulrich, D.P. Tieleman, C. Posten, ^{2}H-NMR study and molecular dynamics simulation of the location, alignment, and mobility of pyrene in POPC bilayers, Biophys. J. 88 (2005) 1818–1827.